NEOPLASIA
www.neoplasia.com

Volume 21 Number 5 May 2019 pp. 469–481 469

Ets1 Plays a Critical Role in MLL/EB1-Mediated Leukemic Transformation in a Mouse Bone Marrow Transplantation Model

Jen-Fen Fu[*], Tzung-Hai Yen[†], Ying-Jung Huang[‡] and Lee-Yung Shih[‡,§]

[*]Department of Medical Research, Chang Gung Memorial Hospital, and Graduate Institute of Clinical Medical Sciences, Chang Gung University, Taoyuan, Taiwan; [†]Department of Nephrology and Poison Center, Chang Gung Memorial Hospital and Chang Gung University, Taoyuan, Taiwan; [‡]Division of Hematology-Oncology, Department of Internal Medicine, Chang Gung Memorial Hospital, Taoyuan, Taiwan; [§]Division of Hematology-Oncology, Department of Internal Medicine, Chang Gung Memorial Hospital, Chang Gung University, Taoyuan, Taiwan

Abstract

Leukemogenic potential of MLL fusion with the coiled-coil domain-containing partner genes and the downstream target genes of this type of MLL fusion have not been clearly investigated. In this study, we demonstrated that the coiled-coil–four-helix bundle structure of EB1 that participated in the *MLL/EB1* was required for immortalizing mouse bone marrow (BM) cells and producing myeloid, but not lymphoid, cell lines. Compared to *MLL/AF10*, *MLL/EB1* had low leukemogenic ability. The *MLL/EB1* cells grew more slowly owing to increased apoptosis *in vitro* and induced acute monocytic leukemia with an incomplete penetrance and longer survival *in vivo*. A comparative analysis of transcriptome profiling between *MLL/EB1* and *MLL/AF10* cell lines revealed that there was an at least two-fold difference in the induction of 318 genes; overall, 51.3% (163/318) of the genes were known to be bound by MLL, while 15.4% (49/318) were bound by both MLL and MLL/AF9. Analysis of the 318 genes using Gene Ontology–PANTHER overrepresentation test revealed significant differences in several biological processes, including cell differentiation, proliferation/programmed cell death, and cell homing/recruitment. The *Ets1* gene, bound by MLL and MLL/AF9, was involved in several biological processes. We demonstrated that *Ets1* was selectively upregulated by *MLL/EB1*. Short hairpin RNA knockdown of *Ets1* in *MLL/EB1* cells reduced the expression of CD115, apoptosis rate, competitive engraftment to BM and spleen, and incidence of leukemia and prolonged the survival of the diseased mice. Our results demonstrated that *MLL/EB1* upregulated *Ets1*, which controlled the balance of leukemia cells between apoptosis and BM engraftment/clonal expansion.

Novelty and impact of this study

The leukemogenic potential of MLL fusion with cytoplasmic proteins containing coiled-coil dimerization domains and the downstream target genes of this type of MLL fusion remain largely unknown. Using a retroviral transduction/transplantation mouse model, we demonstrated that MLL fusion with the coiled-coil–four-helix bundle structure of EB1 has low leukemogenic ability; *Ets1*, which is upregulated by *MLL/EB1*, plays a critical role in leukemic transformation by balance between apoptosis and BM engraftment/clonal expansion.

Neoplasia (2019) 21, 469–481

Abbreviations: aa, amino acid; ALL, acute lymphoblastic leukemia; AML, acute myeloid leukemia; AMoL, acute monocytic leukemia; APC, allophycocyanin; BD, DNA-binding domain; BM, bone marrow; CBC, complete blood cell; CC, coiled-coil; cDNA, complementary DNA; CFC, colony forming capacity; CTD, C-terminal domain; DAPI, 4′,6-diamidino-2-phenylindole; FHB, four-helix bundle; GM-CSF, granulocyte-monocyte colony stimulating factor; H&E, hematoxylin and eosin; IL, interleukin; ip, intraperitoneally; PB, peripheral blood; PBS, phosphate-buffered saline; PCR, polymerase chain reaction; PE, phycoerythrin; PI, propidium iodide; RT, reverse transcription; SCF, stem cell factor; shRNA, short hairpin RNA; WBC, white blood cell; 5-FU, 5-florouracil

Address all correspondence to: Jen-Fen Fu, Ph.D. Department of Medical Research, Chang Gung Memorial Hospital, 5 Fu-Hsing Street, Kwei-San Taoyuan 333, Taiwan. or Lee-Yung Shih, MD, Division of Hematology-Oncology, Department of Internal Medicine, Chang Gung Memorial Hospital, 199 Tung Hwa North Road, Taipei 105, Taiwan. E-mail: cgfujf@cgmh.org.tw
Received 7 January 2019; Revised 7 March 2019; Accepted 12 March 2019

1476-5586
https://doi.org/10.1016/j.neo.2019.03.006

Introduction

Chromosomal rearrangements involving the *MLL* (recently renamed *KMT2A*, also called *ALL1*, *HTRX1*, and *HRX*) gene at 11q23 are detected in patients with acute lymphoid and myeloid leukemias.[1] In general, *MLL* rearrangements are predictive of a poor clinical outcome.[2,3] To date, 135 *MLL* rearrangements have been found in leukemia patients, in whom 94 *MLL* partner genes have been identified.[4] Half of the *MLL* partner genes encode nuclear proteins, and the rest encode cytoplasmic proteins. Among the nuclear partner genes, *AF4* (*AFF1*), *AF9* (*MLLT3*), *ENL* (*MLLT1*), *AF10* (*MLLT10*), or *ELL* accounts for ~80% of cases.[4–7] Structural/functional studies revealed MLL fusion with the transcriptional effector domains of the nuclear proteins involved the recruitment of DOT1L-containing complexes which epigenetically modify the *MLL* target genes and aberrantly sustain their expression.[8] The most well-known MLL and MLL fusion target genes are 5′ *HOXA* (*HOXA7*, *HOXA9*, *HOXA10*) and *MEIS1*. Evidence indicates that overexpression of *Hoxa9* and *Meis1* induces leukemic transformation.[9] Recently, Xu et al. (2016) performed chromatin immunoprecipitation sequencing analysis and identified 5233 MLL1- and 3140 MLL/AF9-binding genes, with 1369 joint targets including 5′ *Hoxa* and *Meis1* genes, in the mouse *MLL/AF9* cells. They also demonstrated that MLL/AF9-binding sites are enriched for the sequences of embryonic or T-cell transcription factors, whereas MLL1 is preferentially recruited to the chromatin regions that are enriched for the consensus sequences of ETS family transcription factors, including ETS1, PU.1, ERG, and ETV1.[10] The transcription factors of ETS family are involved in stem cell development, cell proliferation, survival, and tumorigenesis.[11]

Leukemic transformation induced by MLL fusion with the cytoplasmic fusion partners is less understood. Evidence shows that the coiled-coil dimerization domain of *AF1p* (*EPS15*), *GAS7*, and gephyrin or the self-association domain of *AF6* (*MLLT4*) was required for *MLL* fusion-mediated leukemia development.[12–15] *MLL/AF1p* and *MLL/GAS7* also activated homeobox genes[13]; however, *Hoxa7* and *Hoxa9* were not required for the *MLL/GAS7*-induced leukemic transformation.[16] Thus, the downstream target genes that participate in such a type of *MLL* fusion-induced leukemic transformation remain to be elucidated.

We previously identified a novel *MLL* fusion partner gene, *EB1* (*MAPRE1*), from a patient having *de novo* pro-B acute lymphoblastic leukemia (ALL).[17] *MLL* exhibits 36 exons (NM_005933.3) and *EB1* exhibits 7 exons (NM_012325.3). The resultant MLL/EB1 fusion protein is composed of MLL exons 1 to 8 (aa 1-1362) fused to EB1 exons 6 to 7 (aa 200-268). EB1 is a microtubule plus-end trafficking protein and is involved in cytoskeleton and spindle formation.[18] An examination of the EB1 crystal structure revealed a coiled-coil–four-helix bundle structure at its carboxy-terminal end, and the coiled-coil domain from amino acid [aa] 211 to aa 229 conferred a homo-dimerization activity.[19,20] In this study, we performed retroviral transduction/transplantation and structural/functional assays to investigate the leukemogenic potential of *MLL/EB1*. We also compared transcriptome profiling between the *MLL/EB1* and *MLL/AF10* cell lines as well as identified and investigated the role of the *Ets1* gene, which is selectively upregulated by *MLL/EB1* during *MLL/EB1*-induced leukemic transformation.

Materials and Methods

Plasmid Construction

Total RNA was prepared from patient leukemia cells using Trizol reagent (Gibco BRL, Gaithersburg, MD). Complementary DNA (cDNA) was synthesized from the total RNA by reverse transcription (RT) using oligo-dT and Superscript II reverse transcriptase (Life Technologies, Rockville, MD). The gene fragments of truncated *EB1* (*tEB1*, encoding aa 200-268 of EB1), truncated *MLL* (*tMLL*, encoding aa 1-1362 of MLL), *MLL/EB1* (encoding aa 1-1362 of MLL and aa 200-268 of EB1), *MLL/EB1*ΔαBC (encoding aa 1-1362 of MLL and aa 200-234 of EB1), and *MLL/EB1*ΔαA (encoding aa 1-1362 of MLL and aa 235-268 of EB1) (Figure 1, *A* and *C*) were amplified from a cDNA by performing polymerase chain reaction (PCR) using the Expand Long Template PCR system (Roche Applied Science, Mannheim, Germany). The amplified gene fragments were cloned into the *Eco*RI and *Xho*I sites of the retroviral vector pMSCVneo (Clontech, Palo Alto, CA). Construction of pMSCVneo carrying *MLL/AF10(OM-LZ)* has been described elsewhere. For performing the luciferase reporter assay, the promoter region of *Ets1* (nucleotide [nt] −703 to +293 around the transcription start site of *Ets1* variant 1, NM_011808) (Supplementary Figure 1*A*) was amplified using PCR and cloned into the *Kpn*I and *Bgl*II sites of the luciferase vector pGL4.20 (Promega, Madison, WI) to generate PEts1-luc. The promoter region of human *HOXA7* (nt −1988 to +21 around the transcription start site of *HOXA7*, NM_006896.3) was PCR-amplified and cloned into the *Kpn*I and *Sac*I sites of the luciferase vector pGL2-basic (Promega) to generate PHOXA7-luc. Furthermore, the promoter regions of *HOXA9* (nt −988 to −87 near the transcription start site of *HOXA9*, NM_152739.3) and *MEIS1* (nt −1430 to +453 around the transcription start site of *MEIS1*, NM_002398.2) were cloned into the *Xho*I and *Hind*III sites of pGL2-basic to generate PHOXA9-luc and PMEIS1-luc, respectively. The fidelity of the cloned gene fragments was confirmed by DNA sequencing.

In Vitro Retroviral Transduction/Replating and In Vivo Leukemogenesis Assays

The retroviral production, retroviral transduction of murine BM cells, and intraperitoneal (ip) injection of immortalized BM cell lines into mice were performed as described previously[21] with some modifications. The titer of virus was determined using NIH3T3 cells, and the viral titer of *MLL/EB1* was around 2×10^5/ml. Briefly, the BM cells were prepared from C57BL/6J-Tg(Pgk1-EGFP) 03N male mice (GFP-B6, National Laboratory Animal Center, Taiwan) or C57BL/6J (B6) male mice 5 days after injecting them with 5-florouracil (5-FU; 150 μg/g). BM cells were transduced with retroviruses at an MOI of 1 and selected by replating four times in a methylcellulose medium (M3231, Stem Cell Technologies, Vancouver, BC, Canada) containing lymphoid differentiation-inducing cytokines [20 ng/ml stem cell factor (SCF), 10 ng/ml interleukin 3 (IL3), 10 ng/ml IL7, and 100 ng/ml flt3 ligand] or containing myeloid differentiation-inducing cytokines [20 ng/ml SCF and 10 ng/ml each of IL3, IL6, and granulocyte-monocyte colony stimulating factor (GM-CSF)]. Cells pooled from the colonies grown during the fourth round of plating were adapted to liquid culture [1× RPMI medium containing IL3 (10 ng/ml)]. To determine *in vivo* leukemogenic potential, 1×10^6 immortalized cells or 1.5×10^5-3×10^5 *MLL* fusion-transduced BM cells were ip injected into sublethally irradiated (a dose of 5.25 Gy total-body γ-irradiation) male B6 mice. To monitor leukemia development, peripheral blood (PB) was collected from the transplanted mice every week for complete blood count (CBC) analysis using a hemocytometer (Hemavet 950, Drew Scientific, Oxford, CT).

Phenotypic Analyses

The hematological lineage of mouse BM cells and immortalized cell lines was determined using flow cytometry (FACS-Calibur or CantoII, Becton-Dickinson, Mountain View, CA), which employed phycoerythrin (PE)-Mac1, PE-CD115, PE-CD19, PE-B220, PE-Cy7-c-kit, allophycocyanin (APC)-Sca1, APC-CD3, APC-CD14 (eBioscience, San Diego, CA), and APC-Ly6G (Miltenyi Biotec, Auburn, CA, USA). The liver, spleen, and lymph node collected from the moribund mice were fixed in buffered formalin, embedded in paraffin, sectioned, and stained with hematoxylin and eosin (H&E) using the standard technique. Stamp specimens of the tissues, PB smears, and BM cytospin preparations were stained with Liu reagents (Handsel Technologies, Taipei, Taiwan).

Cell Growth and Apoptosis Analyses

Cell proliferation was evaluated by counting cell numbers every day or by performing WST assay (BioVision, Mountain View, CA). For cell apoptosis analysis, cells were stained with Pacific Blue-conjugated Annexin V (Biolegend, San Diego, CA) and propidium iodide (Annexin V apoptosis detection kit, BD Pharmingen, San Diego, CA) according to the manufacturer's instruction. The stained cells were analyzed immediately using a flow cytometer (FACS-Calibur; Becton-Dickinson).

Luciferase Reporter Assay

32Dcl3 cells, a murine myeloid leukemia cell line, were transfected with pMSCVneo-expressing plasmid [empty vector, *tEB1* (for homeobox genes only), *tMLL*, *MLL/EB1* or *MLL/AF10*] and promoter-luciferase vector (pEts1-luc, pHOXA7-luc, pHOXA9-luc, or pMEIS1-luc) using LT1 liposome (Mirus, Madison, WI). pRL-TK (Promega) was used as an internal control (for homeobox genes only). Cells were harvested at 24 hours after transduction, and luciferase activity was determined using the dual-luciferase assay kit (Promega) and a luminometer (GLOMA X 20/20, Promega).

Microarray Analysis and Gene Ontology–PANTHER Enrichment Analysis

The total RNA of the cells was amplified, labeled, and hybridized to the mouse genome 430 2.0 Array chips (Affymetrix, Santa Clara, CA) by following the manufacturer's instructions (this procedure was performed by the staff of the Genomic Medicine Research Core Laboratory at Chang Gung Memorial Hospital, Linkou, Taiwan). Microarray data are available at NCBI GEO website (accession number: GSE82156). Differentially expressed genes with a fold change of at least two-fold between *MLL/EB1* and *MLL/AF10* cell lines were classified into functional groups of biological process using an online Gene Ontology (GO) enrichment analysis–PANTHER classification system (GO database released 2018-09-06) (http://geneontology.org/page/go-enrichment-analysis). Statistical significance was evaluated using the Fisher's exact test and corrected by Bonferroni correction for multiple testing. The biological process categories of GO having P values of <.05 were considered to be statistically significant.

RT-PCR and Quantitative RT-PCR (RT-qPCR) Analyses

To determine the gene expression level, quantitative PCRs were performed in triplicate using SYBR Green PCR mastermix and analyzed using the ABI Prism 7500 system (Applied Biosystems, Foster City, CA). Primer sets used in PCR were 5′-ATC CAG CTG TGG CAG TTT CTT and 5′-CAC GGC TCA GTT TCT CAT AAT for *Ets1*, 5′-CTG AGT CAG AAG CCC TTC GAC and 5′-CCC AGA CCA AAG GCT GTA GCC for CD115, 5′-CTG AAG GGG GCC TGT ATG TG and 5′-CAT TCT TCG ATT TTG TCT GC for *Cybb*, 5′-CCC ACA GGC AGC ACA GTG GAC and 5′-GGA GGC CGA GGA GGA CCA GG for CD68, and 5′-TTC ACC ACC ATG GAG AAG GC and 5′-GGC ATG GAC TGT GGT CAT GA for *Gapdh*. Gene expression was normalized by calculating the difference between threshold cycle numbers of *Gapdh* and target genes (ΔCt) for each sample. The difference in gene expression level relative to control cells was obtained by calculating the difference between ΔCt of the control and target cell lines (Δ ΔCt). Fold change was calculated as $2^{-\Delta\Delta Ct}$.

To detect which *Ets1* transcription variant was expressed in the cell lines, RT-PCR was performed using the following primer sets: 5′-CGG ACT GGC TGG GCG CGC AC and 5′-GGA GTT AAC AGC GGG ACA TCT for variants 1 and 2 and 5′-ACC CGT CTC TGC AGC AAA TTA and 5′-GGA GTT AAC AGC GGG ACA TCT for variant X1.

Gene Knockdown by shRNA

Lentivirus vector (pLKO_TRC025) and lentivirus that expressed shRNA against mouse *Ets1* (TRCN0000042639 and TRCN0000042642) were obtained from the National RNAi Core Facility Platform (Institute of Molecular Biology/Genomic Research Center, Academia Sinica, Taiwan). Cells were infected with lentivirus in the presence of polybrene (4 μg/ml) for 3 hours; the medium was then replaced with fresh RPMI complete medium, and the cells were cultured for another 24 hours. The infected cells were selected by adding puromycin (2 μg/ml) over a total of 2 weeks. Gene knockdown efficiency in the infected cells was evaluated using RT-qPCR, Western blot, and immunofluorescence labeling.

Immunofluorescence Labeling and Western Blot Analyses

Cytospin preparations of leukemia cells were fixed, permeabilized, and incubated with rabbit polyclonal anti-Ets1 antibody (Santa Cruz Biotechnology, CA); subsequently, the preparations were incubated with FITC-conjugated affinity purified goat anti-rabbit IgG (Jackson Immuno Research, West Grove, PA) and stained with 4′,6-diamidino-2-phenylindole (DAPI). The slides were viewed under a fluorescence microscope BX61 (Olympus, Melville, NY). Western blot analysis was performed as described previously.[22] The primary antibody against mouse β-actin was obtained from Sigma (St Louis, MO). The secondary antibodies, namely, horseradish peroxidase–conjugated anti-mouse IgG and anti-rabbit IgG, were obtained from Jackson Immuno Research Laboratories (West Grove, PA).

In Vivo Competitive Engraftment/Clonal Expansion Assay

To generate a standard curve of cell ratio vs. peak height ratio, ME2G-shEts1 cells and ME2G-shV cells were mixed in ratios of 10:0, 8:2, 6:4, 4:6, 2:8, and 0:10. Genomic DNAs prepared from the cell mixtures were used to amplify the shRNA region via nested PCR. The first round of PCR was performed using the primer set 5′-ACA AAA TAC GTG ACG TAG and 5′-CTG TTG CTA TTA TGT CTA C, whereas the second round of PCR was performed using the primer set 5′-TGG ACT ATC ATA TGC TTA CCG and 5′-CTG TTG CTA TTA TGT CTA C. The PCR products were sequenced using the PCR primer 5′-CTG TTG CTA TTA TGT CTA C, and the peak height of the 99th nucleotide (T for ME2G-shEts1 and G

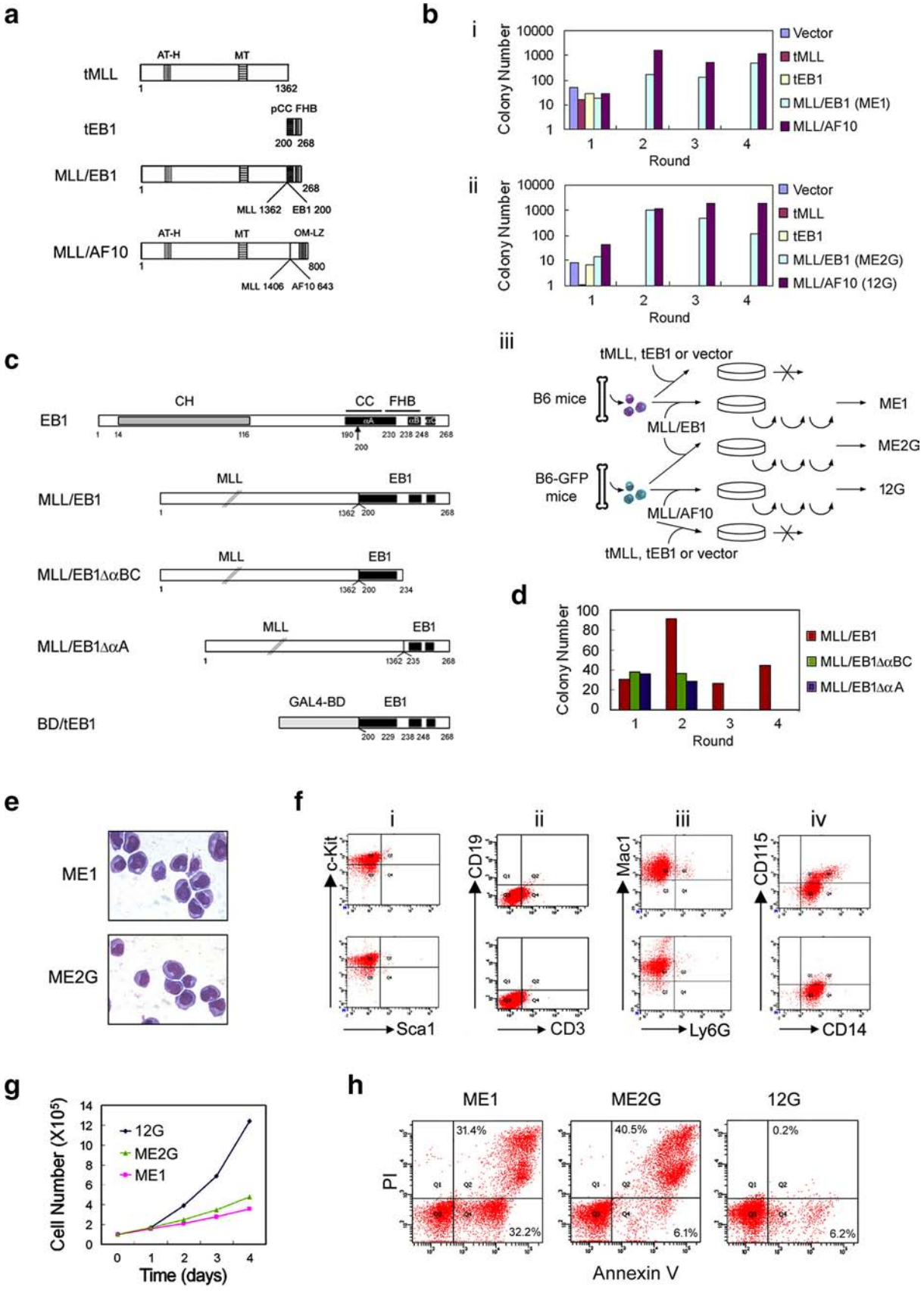
a
tMLL
AT-H
MT
1
1362
tEB1
pCC FHB
200 268
MLL/EB1
268
MLL 1362
EB1 200
MLL/AF10
AT-H
MT
OM-LZ
800
MLL 1406
AF10 643
b
i
Colony Number
Vector
tMLL
tEB1
MLL/EB1 (ME1)
MLL/AF10
Round
ii
Colony Number
Vector
tMLL
tEB1
MLL/EB1 (ME2G)
MLL/AF10 (12G)
Round
iii
tMLL, tEB1 or vector
B6 mice
MLL/EB1
ME1
ME2G
B6-GFP mice
MLL/AF10
12G
tMLL, tEB1 or vector
c
EB1
CH
CC
FHB
MLL/EB1
MLL
EB1
MLL/EB1ΔαBC
MLL/EB1ΔαA
BD/tEB1
GAL4-BD
d
Colony Number
MLL/EB1
MLL/EB1ΔαBC
MLL/EB1ΔαA
Round
e
ME1
ME2G
f
i
ii
iii
iv
c-Kit
Sca1
CD19
CD3
Mac1
Ly6G
CD115
CD14
g
Cell Number (X10⁵)
12G
ME2G
ME1
Time (days)
h
ME1
ME2G
12G
PI
31.4%
32.2%
40.5%
6.1%
0.2%
6.2%
Annexin V

Table 1. Summary of the Phenotypic Features of Mice Transplanted with *MLL/EB1* and *Ets1*-Knockdown *MLL/EB1* Cell Lines

Cell Line	ME1	ME2G	ME2G-shV	ME2G-shEts1
Mouse number	10	14	10	10
Sick mouse number (%)	7 (70%)	13 (93%)	9 (90%)	4 (40%)
Median survival (range) days	260 (116-393)	155 (104-206)	99 (85-120)	264 (213-265)
Median BM blasts/immature form (range)	43.3% (8.4%-49.3%)	82.3% (68.9%-95.3%)	>90%	>90%
Median WBC (range) × 10^3/μl	14.6 (7.2-52.2)	81.5 (33.9-161.5)	67.0 (30.5-118.9)	4.4 (1.2-6.3)
Anemia (%)	4/7 (57.1%)	7/13 (53.8%)	2/7 (28.6%)	2/3 (66.7%)
Thrombocytopenia (%)	6/7 (85.7%)	10/13 (76.9%)	4/7 (57.1%)	2/3 (66.7%)
Hepatosplenomegaly (%)	7/7 (100%)	13/13 (100%)	9/9 (100%)	4/4 (100%)
Enlarged lymph node (%)	3/7 (42.9%)	10/13 (76.9%)	9/9 (100%)	4/4 (100%)
Ascites (%)	3/7 (42.9%)	1/13 (7.7%)	1/9 (11.1%)	0/4 (0%)
Diagnosis	AMoL (M5b-like)	AMoL (M5a-like)	AMoL (M5a-like)	AML

for ME2G-shV; Supplementary Figure 3*A*) was measured. The relationship between cell ratio (ME2G-shEts1/ ME2G-shEts1+ ME2G-shV) and nucleotide peak height ratio (T/T + G) was used to generate the standard curve (Supplementary Figure 3*B*). *In vivo* competitive engraftment/clonal expansion assays were performed as described previously.[23] The mice were sacrificed at 2, 4, 6, 8, and 10 weeks after transplantation (3 mice for each time point). Genomic DNAs were extracted from the initial cell mixture or mice BM and splenic cells, and subsequently nested PCR-DNA sequencing was performed. The cell ratios of ME2G-shEts1/ ME2G-shEts1 + ME2G-shV in the samples were determined by aligning T/T + G peak height ratio to the standard curve.

Ethical Requirements

All animal experiments were approved by the Animal Research Committee of Chang Gung Memorial Hospital and performed in accordance with its guidelines.

Statistical Analyses

Survival analyses were conducted according to the Kaplan-Meier method. Differences in survival were assessed using the log-rank test. Gene expression level was examined via the paired Student's *t* test. *P* values of <.05 were considered to be statistically significant.

Results

MLL/EB1 Expression Immortalizes Mouse BM cells in the Medium Supplemented with Myeloid Differentiation-Inducing Cytokines

To determine the transformation capacity of *MLL/EB1*, we transduced 5-FU–treated BM cells with MSCV carrying *tMLL*, *tEB1*, *MLL/EB1*, or *MLL/AF10(OM-LZ)* (Figure 1*A*) and subsequently evaluated colony-forming capacity (CFC) via a serial replating assay. Our results of three independent experiments showed that BM cells transduced with *MLL/EB1*, *tEB1*, *tMLL*, or *MLL/AF10(OM-LZ)* were unable to form colonies when plated for the second time in the methylcellulose medium supplemented with lymphoid differentiation-inducing cytokines (IL3, IL7, Flt3 ligand). On the contrary, in the medium containing myeloid differentiation-inducing cytokines (IL3, IL6, SCF, and GM-CSF), *MLL/EB1*- and *MLL/AF10(OM-LZ)*-transduced BM cells formed colonies all four rounds of plating in two independent experiments, whereas *tMLL*- and *tEB1*-transduced BM cells did not show any proliferation potential in the second round of plating (Figure 1, *B-i* and *ii*). The *MLL/EB1*-transduced BM cells had a lower CFC than that of *MLL/AF10(OM-LZ)*-transduced BM cells at rounds three and four of plating (Figure 1*B*).

The carboxy-terminal end of EB1 consists of the three α-helices, αA (aa 190-230), αB (aa 238-248), and αC (aa 251-254) (Figure 1*C*). The αA and αB helices form a coiled coil (CC)–four-helix bundle (FHB) structure (Figure 1*C*), which mediates EB1 homo-dimerization.[20] To investigate whether both CC (aa 200-230) and FHB were required for MLL/EB1-mediated BM cell transformation, the two constructs αA-deleted *MLL/EB1* (MLL/EB1ΔαA) and αB-αC-deleted *MLL/EB1* (MLL/EB1ΔαBC) were generated (Figure 1*C*). Data of retroviral transduction/replating assay showed that the BM cells transduced with both types of deletion constructs ran out of proliferation potential in the second round of plating (Figure 1*D*), suggesting that both CC and FHB are required for *MLL/EB1*-induced cell transformation.

Two cell lines, ME1 and ME2G, were generated from the independent retroviral transduction/replating assays (Figure 1*E*). Both ME1 and ME2G cells showed a blastic morphology with a high

Figure 1. Establishment and characterization of the *MLL/EB1*-immortalized cell lines. (A) Schematic representations of truncated *MLL* (tMLL), truncated EB1 (tEB1), MLL/EB1, and MLL/AF10(OM-LZ) fusion proteins. AT-H, AT hooks; MT, DNA methyltransferase domain; pCC, partial coiled coil domain; FHB, four-helix bundle; OM, octapeptide motif; LZ, leucine zipper. The numbers indicate the amino acid of each protein. (B) Transduction efficiency of the blank retrovirus (Vector) or retroviruses expressing tMLL, tEB1, MLL/EB1, and MLL/AF10(OM-LZ) in two independent experiments using B6 (i) or B6-GFP mice BM cells (ii). The bars indicate the colonies generated per 3×10^4 transduced murine BM cells. MLL/AF10(OM-LZ) was used as a positive control. ME1 and ME2G were *MLL/EB1*-immortalized cell lines generated by adaptation of the cells, which were pooled from the fourth round of plating, to liquid culture (iii). 12G was the *MLL/AF10(OM-LZ)*-immortalized cell line (iii). (C) Schematic representation of EB1, MLL/EB1, MLL/EB1 αBC, and MLL/EB1 αA. CH, calponin homology domain; CC, coiled coil domain; FHB, four-helix bundle; αA, αB, and αC, the three α-helices of EB1. (D) Transduction efficiency of the retroviruses expressing truncated and fusion genes. The bars indicate the colonies generated per 1×10^4 transduced mouse BM cells. (E) Liu staining of the *MLL/EB1*-immortalized cell lines cultured in the medium containing IL3 (oil immersion, ×1000). (F) Immunophenotypic analysis of the *MLL/EB1*-immortalized cell lines [upper panel (ME1), lower panel (ME2G)]. (G) Growth curve of the *MLL/EB1*-immortalized cell lines (ME1 and ME2G) and *MLL/AF10(OM-LZ)*-immortalized cell line (12G) in the medium containing IL3. (H) Flow cytometry analysis of live and apoptotic cells by staining with Annexin V and propidium iodide (PI).

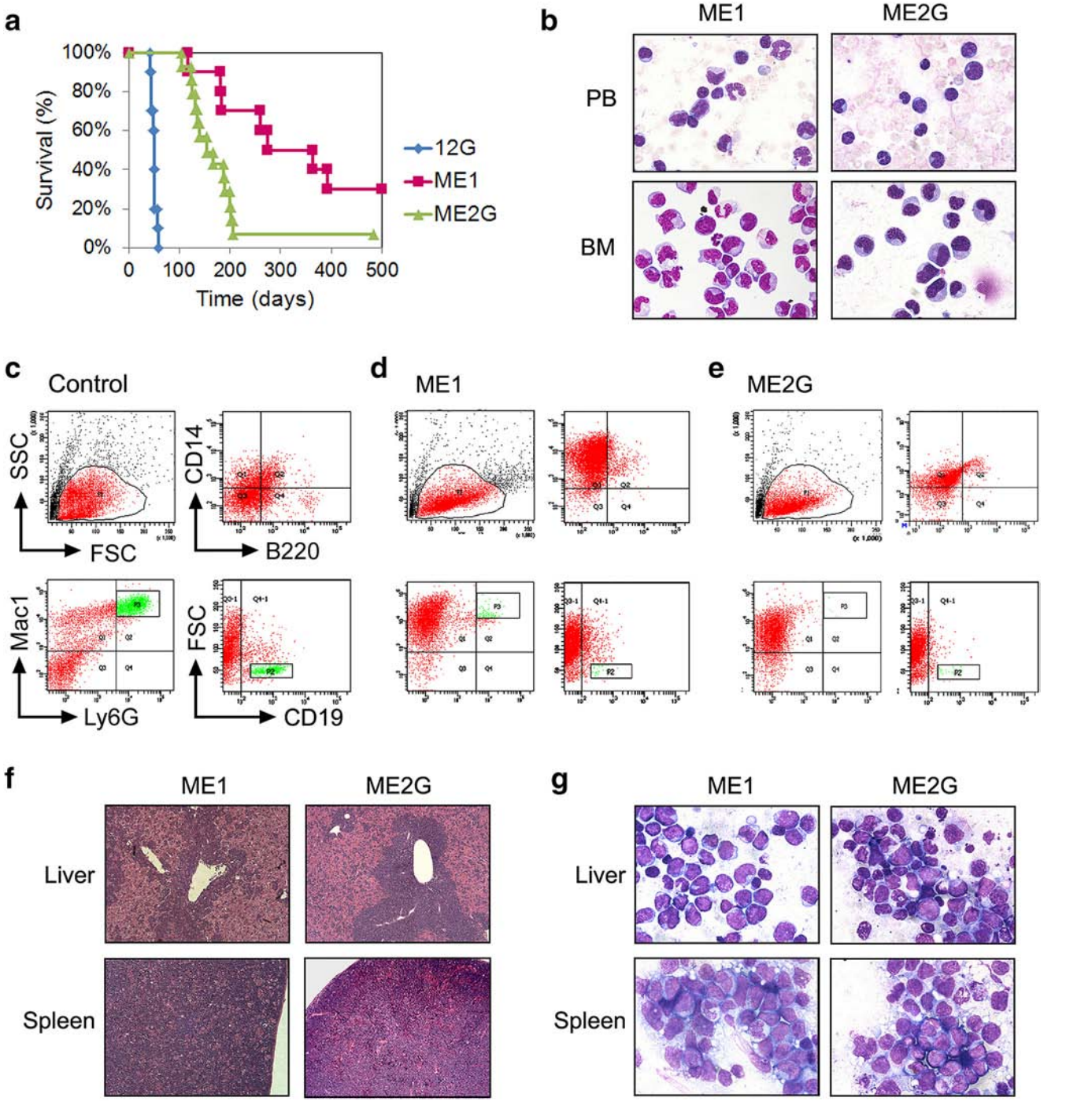

Figure 2. Characteristics of the leukemia mice transplanted with the *MLL/EB1*-immortalized cell lines. (A) Survival curves of the sublethally irradiated mice which were ip injected with ME1 or ME2G cells. Mice injected with 12G cells were used as the positive control (data has been shown in ref. [21]). (B) Liu staining of PB smears or cytospin preparations of BM cells from the representative leukemic mice (oil immersion, ×1000). (C-E) Flow cytometric analysis of hematopoietic subsets in the BM cells of control mouse (C), representative (D) ME1- and (E) ME2G-leukemic mice. (F) Histological sections of the liver and spleen of the representative leukemic mice (H&E staining, ×100). (G) Stamp smears of the liver and spleen of the representative leukemic mice (Liu staining, oil immersion, ×1000).

nucleus-to-cytoplasm ratio in the medium containing IL3 (Figure 1*E*). Immunophenotypic analysis of ME1 and ME2G cells revealed the following expression patterns for both cell types: c-kit hematopoietic progenitor cell marker expression without Sca1 hematopoietic stem cell marker expression (Figure 1, *F-i*); dim CD3 T cell marker expression without CD19 B lymphocyte marker expression (Figure 1, *F-ii*); Mac1 myeloid lineage marker expression without Ly6G granulocyte marker expression (Figure 1, *F-iii*); and CD14 monocytic marker expression, with only 17.7% of the ME1 cells expressing monocytic lineage marker CD115 (Figure 1, *F-iv*); this observation indicated that *MLL/EB1* mediated the immortalization of mouse BM cells along the monocytic lineage.

Compared with 12G cells, *MLL/AF10(OM-LZ)*-immortalized cells, ME1, and ME2G cells had lower growth rates in the

IL3-containing medium (Figure 1*G*). The high percentages of cells in the early and late apoptotic stages [32.2% and 31.4% (ME1) and 6.1% and 40.5% (ME2G) vs. 6.2% and 0.2% (12G)] (Figure 1*H*) indicated that *MLL/EB1* had a higher potential to induce apoptosis than *MLL/AF10(OM-LZ)*.

MLL/EB1 Induced Acute Monocytic Leukemia with Low Penetrance and Longer Survival

To assess the *in vivo* leukemogenic potential of *MLL/EB1*, 5-FU–treated BM cells were retrovirally transduced with *MLL/EB1* or *MLL/AF10(OM-LZ)*, followed by a direct ip injection of the cells into B6 mice. The mouse injected with the *MLL/AF10(OM-LZ)*-transduced BM cells developed MPN-like myeloid leukemia within 12 weeks, whereas none of the mice injected with the *MLL/EB1*-transduced BM cells developed leukemia [a total of 7 mice, 2 were injected with a dose of 1.5×10^5 BM cells/mouse (observation time 54 weeks) and 5 were injected with a dose of 3×10^5 BM cells/mouse (observation time 2 years)]. These results suggested that *MLL/EB1* had a lower leukemogenic potential than *MLL/AF10(OM-LZ)*.

We subsequently assessed the leukemogenic potential of ME1, ME2G, and control (12G) cell lines. Seven of the 10 (70%) mice injected with ME1 cells and 13 of the 14 (93%) mice injected with ME2G cells developed leukemia (Table 1 and Figure 2*A*). Leukemic ME1 and ME2G mice had significantly longer median survivals than the leukemic 12G mice [260 (range 116-393) days and 155 (range 104-206) days vs. 50 days[21]] (12G vs. ME1 $P < .005$; 12G vs. ME2G $P < .0001$; ME1 vs. ME2G $P < .05$) (Figure 2*A*). Most of the leukemic mice showed hyperleukocytosis, but ME1 mice had a lower median white blood cell (WBC) count than the ME2G mice (14.6×10^3/μl vs. 81.5×10^3/μl) before moribund (Table 1). The time from the appearance of leukocytosis in PB to moribund was usually <3 weeks. ME1 and ME2G mice had 43.3% and 82.3% immature forms/blasts in BM, respectively (Table 1 and Figure 2*B*). Immunophenotypic analysis of the mouse BM cells revealed lower levels of $CD19^+$ /$B220^+$ B-lymphocytes and $Ly6G^+$ granulocytes in ME1 and ME2G mice than those in control mice, indicating suppression of B-cell lymphopoiesis and granulopoiesis of the recipient BM by ME1/ME2G cells (Figure 2, *C-E*). The leukemic cells of ME1 mice expressed brilliant Mac1 and CD14, which were moderately expressed in ME2G mice (Figure 2, *D-E*). The cytological and immunophenotypic findings showed that the leukemic cells of ME1 and ME2G mice had varied levels of monocytic maturation. Both ME1 and ME2G mice developed anemia (57.1% vs. 53.8%) and thrombocytopenia (85.7% vs. 76.9%) at similar rates (Table 1). All of the leukemic ME1 and ME2G mice had hepatosplenomegaly (Table 1). Compared with the ME2G mice, ME1 mice had a lower frequency of enlarged lymph nodes but a higher frequency of ascites (Table 1). Pathological examination showed that the periportal region of the liver was infiltrated with leukemia cells; the architecture of the red and white pulps of the spleen was disrupted by leukemia cells (Figure 2*F*). Liu-staining of the stamp smears showed that both the liver and spleen were infiltrated with leukemic blasts (Figure 2*G*). According to the Bethesda proposals for the classification of murine nonlymphoid hematopoietic neoplasms,[24] *MLL/EB1* induced acute monocytic leukemia (AMoL), namely, M5b-like for ME1 mice and M5a-like for ME2G mice.

MLL/EB1 Cells Had Higher Ets1 Expression Level

The leukemic transformation induced by *MLL/EB1* was different from that induced by *MLL/AF10(OM-LZ)*. To identify *MLL/EB1*-specific downstream target gene(s) involved in leukemic transformation, we compared the transcriptome between 12G and ME1/ME2G cell lines on the basis of cDNA microarray data. Sixty-four upregulated (≥2-fold) and 254 downregulated (≤0.5-fold) genes were identified in both ME1 and ME2G as opposed to the 12G cells (Figure 3*A*). Among these 318 differentially expressed genes, 163 genes (49 upregulated and 114 downregulated) have been reported to be MLL-bound genes, and 49 (13 upregulated and 36 downregulated) were joint targets of MLL1 and MLL/AF9[10] (Figure 3*A*). The GO biological process terms that were overrepresented in the 318 genes included several terms related to cell proliferation/apoptosis, namely, "negative regulation of cell proliferation (GO:0008285)," "regulation of programmed cell death (GO:0043067)"; cell differentiation, namely, "regulation of leukocyte differentiation (GO:1902105)," "positive regulation of cell differentiation (GO:0045597)," "cell differentiation (GO:0030154)"; cell homing/engraftment, namely, "positive regulation of cell migration (GO:0030335)," "positive regulation of cell adhesion (GO:0045785)," "chemotaxis (GO:0006953)"; and inflammatory response, namely, "regulation of inflammatory response (GO:0050727)," "inflammatory response (GO:0006954)," "immune system process (GO:0002376)" (Figure 3*B*). The enrichment in these biological processes is consistent with the observations that ME1/ME2G and 12G cells were different in terms of their leukemogenic potential as well as cell differentiation and proliferation ability.

Among the 64 upregulated genes, *Ets1*, which is bound by MLL1 and MLL/AF9, was seen to be involved in the GO biological processes of inflammatory/immune system, cell migration/adhesion, differentiation, and programmed cell death (Figure 3*B*). The RT-qPCR and Western blot analyses confirmed that *Ets1* expression level was higher in ME1/ME2G than in 12G cells (Figure 3, *C-i* and *ii*). Immunofluorescence labeling illustrated the presence of more nuclear Ets1 protein in ME1/ME2G cells than in 12G cells (Figs. 3*D*). To determine whether the high expression level of *Ets1* was induced by *MLL/EB1* fusion, we performed luciferase reporter assay. Transcription of *Ets1* is controlled by two promoters (Supplementary Figure 1*A*). The proximal promoter generates *Ets1* variants 1 and 2, whereas the distal promoter generates variant X1. RT-PCR analysis revealed that the variant X1 was not expressed in our leukemic cell lines (Supplementary Figure 1*B*). Therefore, only a region that spans the transcription start site of variant 1/2 (nt −703 to +293) (Supplementary Figure 1*A*) was cloned into a luciferase reporter plasmid. Our results showed that the *Ets1* promoter-driven luciferase activity was upregulated by *MLL/EB1* but not by *MLL/AF10(OM-LZ)* or *tMLL* (Figure 3*E* and supplementary Figs. 1, *C-E*), suggesting that *Ets1* was selectively upregulated by *MLL/EB1*.

The 318 differentially expressed genes did not include 5′ *Hoxa* (*Hoxa7*, *Hoxa9*, *Hoxa10*) and *Meis1* (Figure 3*A*). We performed luciferase reporter assays and demonstrated that *HOXA7*, *HOXA9*, and *MEIS1* promoter-driven luciferase activities were upregulated by both *MLL/EB1* and *MLL/AF10(OM-LZ)* (Supplementary Figs. 2, *A-C*), indicating that *MLL/EB1*, like *MLL/AF10* and other *MLL* fusions, activated 5′ *HOXA* and *MEIS1* genes.

Knockdown of Ets1 Expression Reduced Cell Monocytic Differentiation and Apoptosis

To investigate the role of *Ets1* in the monocytic differentiation and apoptosis of *MLL/EB1* cells, we transduced two lentivirus-based

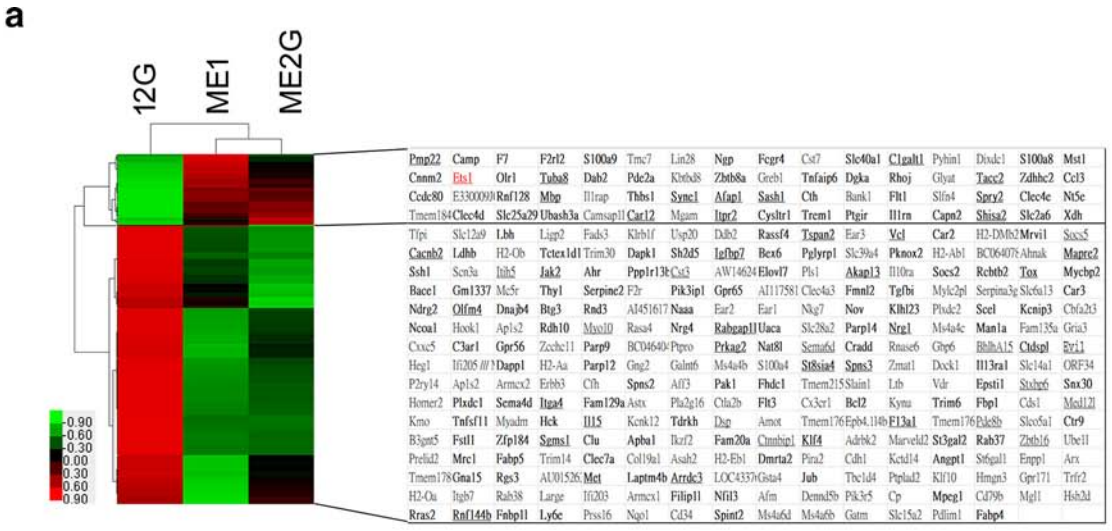
a
12G
ME1
ME2G
-0.90
-0.60
-0.30
0.00
0.30
0.60
0.90
Pmp22 Camp F7 F2rl2 S100a9 Trnc7 Lin28 Ngp Fcgr4 Cst7 Slc40a1 C1galt1 Pyhin1 Dixdc1 S100a8 Mst1
Cnnm2 Ets1 Olr1 Tuba8 Dab2 Pde2a Kbtbd8 Zbtb8a Grebl Tnfaip6 Dgka Rhoj Glyat Tacc2 Zdhhc2 Ccl3
Ccdc80 E330009J Rnf128 Mbp Il1rap Thbs1 Sync1 Afap1 Sash1 Cth Bank1 Flt1 Slfn4 Spry2 Clec4e Nt5e
Tmem184 Clec4d Slc25a29 Ubash3a Camsap1l Car12 Mgam Itpr2 Cysltr1 Trem1 Ptgir Il1rn Capn2 Shisa2 Slc2a6 Xdh
Tfpi Slc12a9 Lbh Ligp2 Fads3 Klrb1f Usp20 Ddb2 Rassf4 Tspan2 Ear3 Vcl Car2 H2-DMb2 Mrvi1 Socs5
Cacnb2 Ldhb H2-Ob Tctex1d1 Trim30 Dapk1 Sh2d5 Igfbp7 Bex6 Pglyrp1 Slc39a4 Pknox2 H2-Ab1 BC064078 Ahnak Mapre2
Ssh1 Scn3a Itih5 Jak2 Ahr Ppp1r13b Cst3 AW14624 Elovl7 Pls1 Akap13 Il10ra Socs2 Rcbtb2 Tox Mycbp2
Bace1 Gm1337 Mc5r Thy1 Serpinc2 F2r Pik3ip1 Gpr65 AI117581 Clec4a3 Fmnl2 Tgfbi Mylc2pl Serpina3g Slc6a13 Car3
Ndrg2 Olfm4 Dnajb4 Btg3 Rnd3 AI451617 Naaa Ear2 Ear1 Nkg7 Nov Klhl23 Ptvdc2 Scel Kcnip3 Cbfa2t3
Ncoa1 Hook1 Ap1s2 Rdh10 Myo10 Rasa4 Nrg4 Rabgap1l Uaca Slc28a2 Parp14 Nrg1 Ms4a4c Man1a Fam135a Gria3
Cxxc5 C3ar1 Gpr56 Zcchc11 Parp9 BC04640 Ptpro Prkag2 Nat8l Sema6d Cradd Rnase6 Gbp6 BhlhA15 Ctdspl Ryl1
Heg1 Ifi205 /// Dappl H2-Aa Parp12 Gng2 Galnt6 Ms4a4b S100a4 St8sia4 Spns3 Zmat1 Dock1 Il13ra1 Slc14a1 ORF34
P2ry14 Ap1s2 Armcx2 Erbb3 Cfh Spns2 Aif3 Pak1 Fhdc1 Tmem215 Slain1 Ltb Vdr Epsti1 Stxbp6 Snx30
Homer2 Plxdc1 Sema4d Itga4 Fam129a Astx Pla2g16 Cila2b Flt3 Cx3cr1 Bcl2 Kynu Trim6 Fbp1 Cds1 Mod1l
Kmo Tnfsf11 Myadm Hck Il15 Kcnk12 Tdrkh Dsp Amot Tmem176 Epb4.1l4b Fl3a1 Tmem176 Pde8b Slco5a1 Ctr9
B3gnt5 Fstl1 Zfp184 Sgms1 Clu Apba1 Ikzf2 Fam20a Ctnnbip1 Klf4 Adrbk2 Marveld2 St3gal2 Rab37 Ztbtb16 Ube1l
Prelid2 Mrc1 Fabp5 Trim14 Clec7a Col19a1 Asah2 H2-Eb1 Dmrta2 Pira2 Cdh1 Kctd14 Angpt1 Stfgal1 Enpp1 Arx
Tmem178 Gna15 Rgs3 AU01526 Met Laptm4b Arrdc3 LOC4337 Gsta4 Jub Tbc1d4 Ptplad2 Klf10 Hmgn3 Gpr171 Trfr2
H2-Oa Itgb7 Rab38 Large Ifi203 Armcx1 Filip1l Nfil3 Afm Dennd5b Pik3r5 Cp Mpeg1 Cd79b Mgl1 Hsh2d
Rras2 Rnf144b Fnbp1l Ly6c Prss16 Nqo1 Cd34 Spint2 Ms4a6d Ms4a6b Gatm Slc15a2 Pdlim1 Fabp4

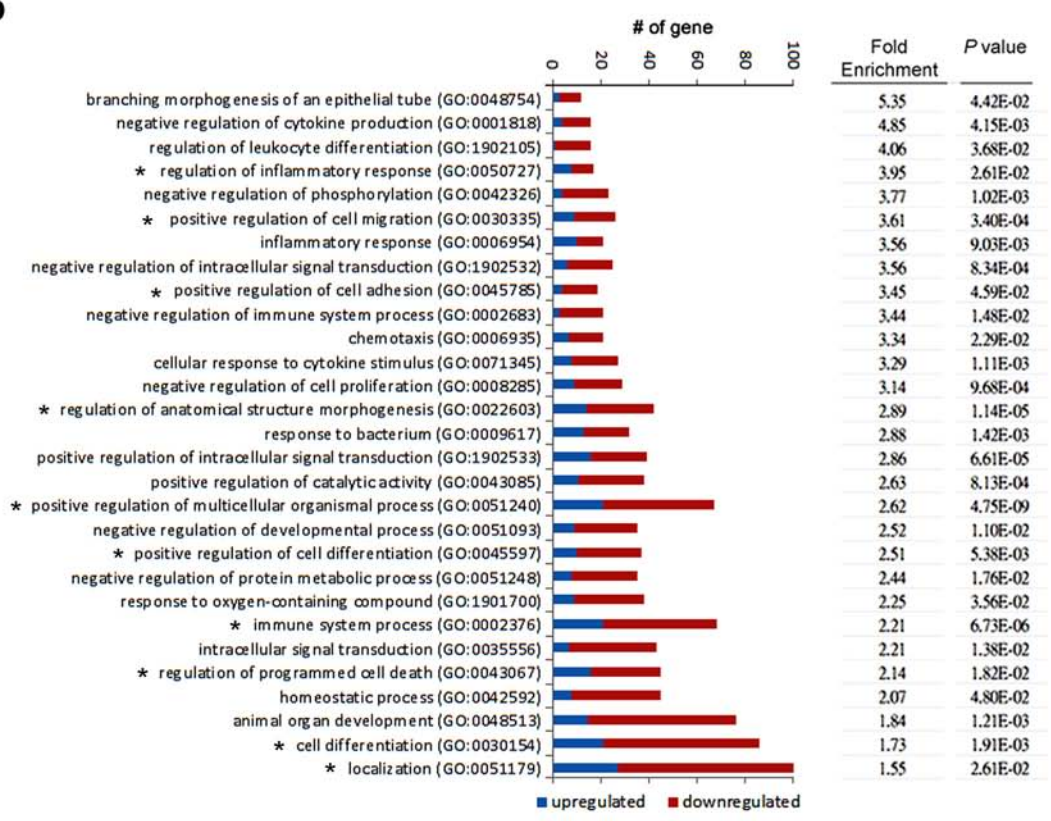
b
# of gene
0 20 40 60 80 100
Fold Enrichment
P value
branching morphogenesis of an epithelial tube (GO:0048754) 5.35 4.42E-02
negative regulation of cytokine production (GO:0001818) 4.85 4.15E-03
regulation of leukocyte differentiation (GO:1902105) 4.06 3.68E-02
* regulation of inflammatory response (GO:0050727) 3.95 2.61E-02
negative regulation of phosphorylation (GO:0042326) 3.77 1.02E-03
* positive regulation of cell migration (GO:0030335) 3.61 3.40E-04
inflammatory response (GO:0006954) 3.56 9.03E-03
negative regulation of intracellular signal transduction (GO:1902532) 3.56 8.34E-04
* positive regulation of cell adhesion (GO:0045785) 3.45 4.59E-02
negative regulation of immune system process (GO:0002683) 3.44 1.48E-02
chemotaxis (GO:0006935) 3.34 2.29E-02
cellular response to cytokine stimulus (GO:0071345) 3.29 1.11E-03
negative regulation of cell proliferation (GO:0008285) 3.14 9.68E-04
* regulation of anatomical structure morphogenesis (GO:0022603) 2.89 1.14E-05
response to bacterium (GO:0009617) 2.88 1.42E-03
positive regulation of intracellular signal transduction (GO:1902533) 2.86 6.61E-05
positive regulation of catalytic activity (GO:0043085) 2.63 8.13E-04
* positive regulation of multicellular organismal process (GO:0051240) 2.62 4.75E-09
negative regulation of developmental process (GO:0051093) 2.52 1.10E-02
* positive regulation of cell differentiation (GO:0045597) 2.51 5.38E-03
negative regulation of protein metabolic process (GO:0051248) 2.44 1.76E-02
response to oxygen-containing compound (GO:1901700) 2.25 3.56E-02
* immune system process (GO:0002376) 2.21 6.73E-06
intracellular signal transduction (GO:0035556) 2.21 1.38E-02
* regulation of programmed cell death (GO:0043067) 2.14 1.82E-02
homeostatic process (GO:0042592) 2.07 4.80E-02
animal organ development (GO:0048513) 1.84 1.21E-03
* cell differentiation (GO:0030154) 1.73 1.91E-03
* localization (GO:0051179) 1.55 2.61E-02
upregulated
downregulated

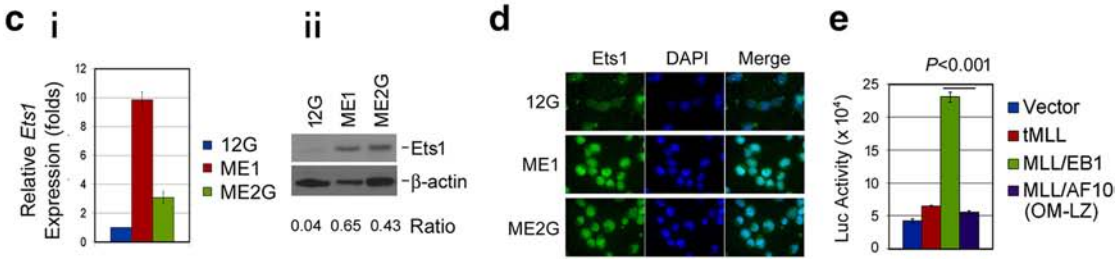
c i
Relative Ets1 Expression (folds)
0 2 4 6 8 10 12
12G
ME1
ME2G
ii
12G ME1 ME2G
Ets1
β-actin
0.04 0.65 0.43 Ratio
d
Ets1 DAPI Merge
12G
ME1
ME2G
e
P<0.001
Luc Activity (x 10⁴)
0 5 10 15 20 25
Vector
tMLL
MLL/EB1
MLL/AF10 (OM-LZ)

shRNAs against *Ets1* into ME1 and ME2G cells to generate *Ets1*--knockdown cell lines. RT-qPCR analysis showed that, as opposed to the cells transduced with empty lentiviruses, *Ets1* expression levels were reduced to 29% (ME1-shEts1) and 23% (ME2G-shEts1) owing to transduction with shRNA TRCN0000042639 (Figure 4, *A-i*). The second shRNA clone TRCN0000042642 failed to generate *Ets1*--knockdown cell lines. Because of the low penetrance of leukemia (please see below), we did not further analyze ME1-shEts1 cells. Reduction of Ets1 protein level in ME2G-shEts1 cells was confirmed by Western blot analysis (Figure 4, *A-ii*). Immunofluorescence labeling further confirmed that the level of Ets1 protein was substantially decreased in the nuclei of ME2G-shEts1 cells (Figure 4*B*). Both ME2G-shV and ME2G-shEts1 cells had a blastic morphology; however, ME2G-shEts1 cells were enlarged (Figure 4*C*). ME2G-shEts1 cells showed high forward and side light scatters, consistent with their large size (Figure 4, *D-i*). The expression of the hematopoietic lineage markers, including Sca1, c-Kit, CD19, CD3, Mac1, Ly6G, and CD14, in ME2G-shV and ME2G-shEts1 cell lines remained the same as that in their parental ME2G cells (Figures 4*D* and 1*D*). However, ME2G-shEts1 cells had decreased expression of the monocytic lineage marker CD115 (Figure 4, *D-v*), as confirmed by RT-qPCR analysis (Figure 4*E*). Moreover, the expression levels of mature monocytic markers *Cybb* and CD68 were also decreased in ME2G-shEts1 cells (Figure 4*E*). M-CSF treatment induced the generation of macrophage-like cells from ME2G-shV but not ME2G-shEts1 cells, which continued to have a blastic morphology (Figure 4*F*). These results indicated that knockdown of *Ets1* expression in *MLL/EB1* cells reduced monocytic differentiation and blocked M-CSF–induced macrophage development.

ME2G-shEts1 cells had a higher growth rate (Figure 4*G*) and a lower percentage of cells at the late apoptotic stage (33.8% vs. 40.9%) than ME2G-shV cells (Figure 4*H*), indicating that knockdown of *Ets1* expression reduces the frequency of *MLL/EB1* cell apoptosis.

Knockdown of Ets1 Expression in MLL/EB1 Cells Impaired Cell Engraftment to BM/Spleen and Leukemia Development

To investigate the role of *Ets1* in *MLL/EB1*-mediated leukemia development, we first compared the *in vivo* competitive engraftment/clonal expansion activity between ME2G-shEts1 and ME2G-shV cells. By aligning with the standard curve for cell ratio vs. allele burden (Supplementary Fig. 3, *A* and *B*), we showed that ME2G-shEts1 cells were poorly engrafted/expanded in the BM and spleen of the recipient mice because the shRNA region of none of the ME2G-shEts1 cells was amplified from the samples collected at 2, 4, 6, 8, and 10 weeks after transplantation (Figure 5, *A-B* and Supplementary Figure 3*C*). These results indicated that knockdown of *Ets1* expression severely impaired *in vivo* engraftment activity of MLL/EB1 cells despite reducing the frequency of cell apoptosis.

We also performed a BM transplantation assay to determine the leukemogenesis of *Ets1*-knockdown *MLL/EB1* cells. None of the six mice injected with ME1-shEts1 cells developed AML, whereas one of the six mice injected with ME1-shV developed AML before the experiment ended (335 days). On the other hand, only 4/10 (40%) mice injected with ME2G-shEts1 cells developed AML, whereas 9/10 (90%) mice transplanted with ME2G-shV cells developed AMoL (Table 1 and Figure 5*C*). The median survival of the leukemic ME2G-shEts1 mice was significantly longer than leukemic ME2G-shV mice (264 days vs. 99 days, $P < .01$) (Table 1). The PB of ME2G-shV mice at moribund stage showed hyperleukocytosis with a median WBC count (comprising lymphocytes and leukemia blasts) of $67.0 \times 10^3/\mu l$, whereas the leukemic ME2G-shEts1 mice showed pancytopenia or a normal WBC count, with a median WBC count (exclusively comprising lymphocytes) of $4.4 \times 10^3/\mu l$ (Figure 5*D* upper panel and Table 1). At moribund stage, >90% of the BM cells from ME2G-shV and ME2G-shEts1 mice were immature forms/blasts (Table 1), but ME2G-shEts1 mice had a larger size of blast cells with a minimal CD115 expression rate (Figure 5*D*, *E-i* and *E-v*). Both ME2G-shV and ME2G-shEts1 mice showed a rare occurrence of $CD19^+$ B lymphocytes and $Ly6G^+$ granulocytes (Figure 5, *E-iii* and *iv*), indicating that *Ets1*-knockdown ME2G cells retain the ability to suppress recipient B-cell lymphopoiesis and granulopoiesis *in vivo*. Compared with leukemic ME2G-shV mice, leukemic ME2G-shEts1 mice had a higher incidence rate of anemia (66.7% vs. 28.6%) but a similar rate of thromobocytopenia (66.7% vs. 57.1%); however, both mice had the same degree of hepatosplenomegaly (100% vs. 100%) and lymph node enlargement (100% vs. 100%) (Table 1). One of the ME2G-shV mice had ascites (11.1% vs. 0%) (Table 1). Taken together, our results demonstrated that the knockdown of *Ets1* expression reduced *MLL/EB1*-induced leukemia development and prolonged the survival of leukemic mice *in vivo*.

Discussion

Previous studies have revealed that the carboxy-terminal end of EB1 contained a coiled-coil–four-helix bundle structure that conferred dimerization activity.[19,20] In this study, we demonstrated that MLL fusion between both the coiled-coil and four-helix bundle structure is required for facilitating the immortalization of murine BM cells. Our results further supported that the N-terminal MLL fused to the coiled-coil dimerization domain is leukemogenic.[12,13] However, while *MLL/AF10*-transduced BM cells (1.5×10^5 /mouse) induced

Figure 3. Ets1 is overexpressed in *MLL/EB1* cell lines. (A) Heat-map and list of the 318 genes differentially expressed in the transcriptome profiling of *MLL/EB1* cell lines (ME1 and ME2G) in comparison with the *MLL/AF10* cell line (12G). Hierarchical clustering was performed and heat-map was obtained using Cluster 3.0 and TreeView1.1.6r4. Raw values were log2-transformed and centered relative to the median. Red indicates that the level of gene expression is higher than the median, and green indicates that the level is lower than the median. The known MLL1-bound genes are indicated in bold type; genes that were jointly bound to both MLL1 and MLL/AF9 are underlined. (B) Enriched biological process Gene Ontology (GO) terms for the 318 differentially expressed genes. All GO terms listed on the bar plot show significant enrichment ($P < .05$). Fold enrichment refers to the number of genes represented in each category relative to the random expression of all genes in the human genome. Bars indicate gene counts; blue and red bars indicate the upregulated and downregulated genes, respectively. The GO biological processes involving *Ets1* gene are indicated by *. (C) RT-qPCR (i) and Western blot (ii) analyses of *Ets1* expression level in 12G, ME1, and ME2G cells. Error bars indicate the standard deviation (SD) of mean. (D) Immunofluorescence staining of 12G, ME1, and ME2G cells with Ets1 (green, left column) and DAPI (blue, middle column). The merged images were shown in the right column. (E) Luciferase reporter analysis. 32Dcl3 cells were transduced with *Ets1* promoter-reporter construct, PEts1-luc, and retrovirus empty vector or vector-carrying *tMLL*, *MLL/EB1*, or *MLL/AF10(OM-LZ)* plasmid DNA. Graph shows a representative result from four individual assays. Error bars represent SD.

MPN-like myeloid leukemia in the recipient mice, *MLL/EB1*-transduced BM cells (1.5×10^5-3×10^5 BM cells/mouse) failed to induce leukemia. The retroviral transduction/replating assay also showed lower CFC of *MLL/EB1*-transduced cells than that of *MLL/AF10(OM-LZ)*-transduced cells. These results suggested that the leukemogenic potential of *MLL/EB1* was lower than that of *MLL/AF10*.

Our patient with *MLL/EB1* was diagnosed as having pro-B ALL, but the transduction of *MLL/EB1* did not immortalize murine BM

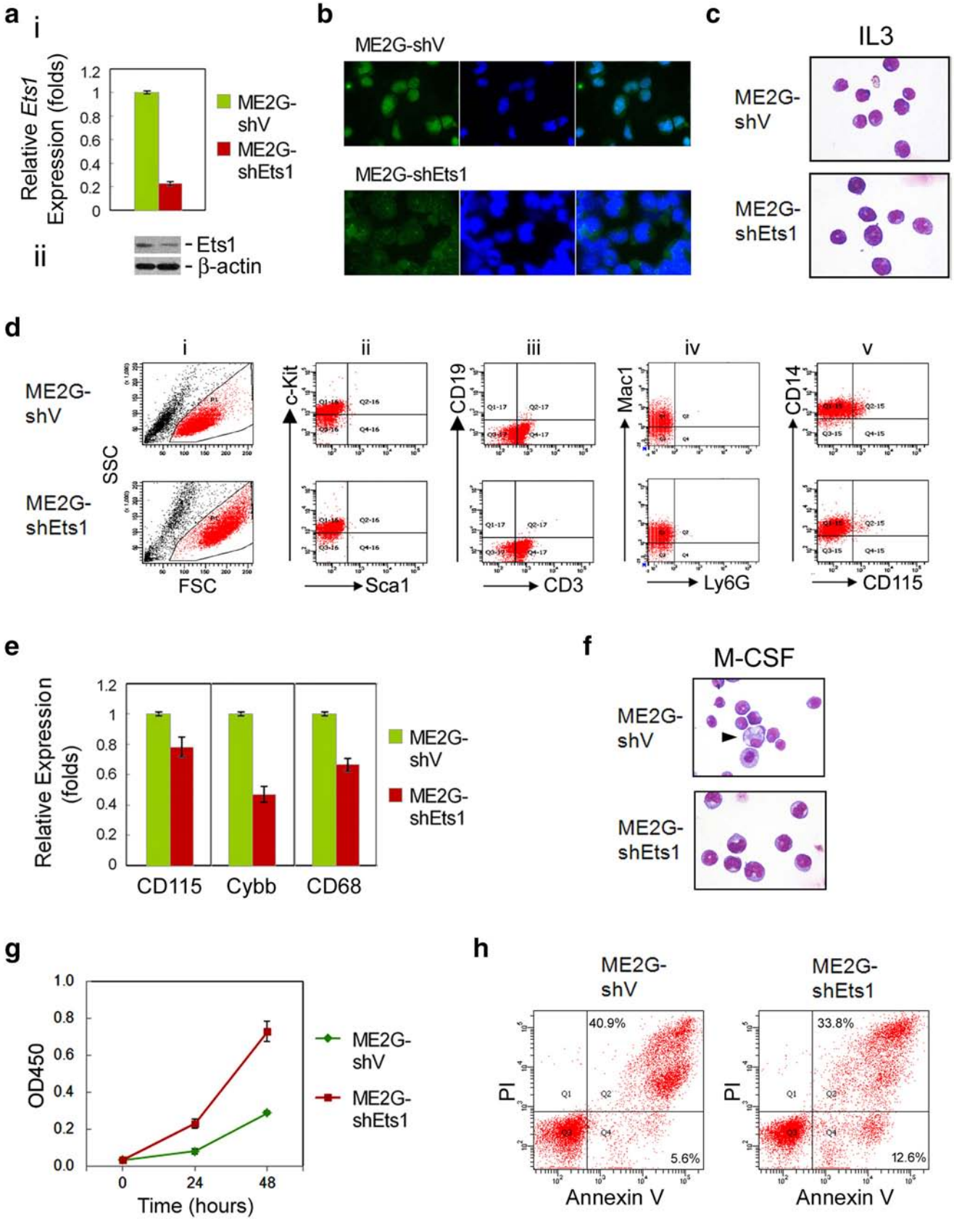

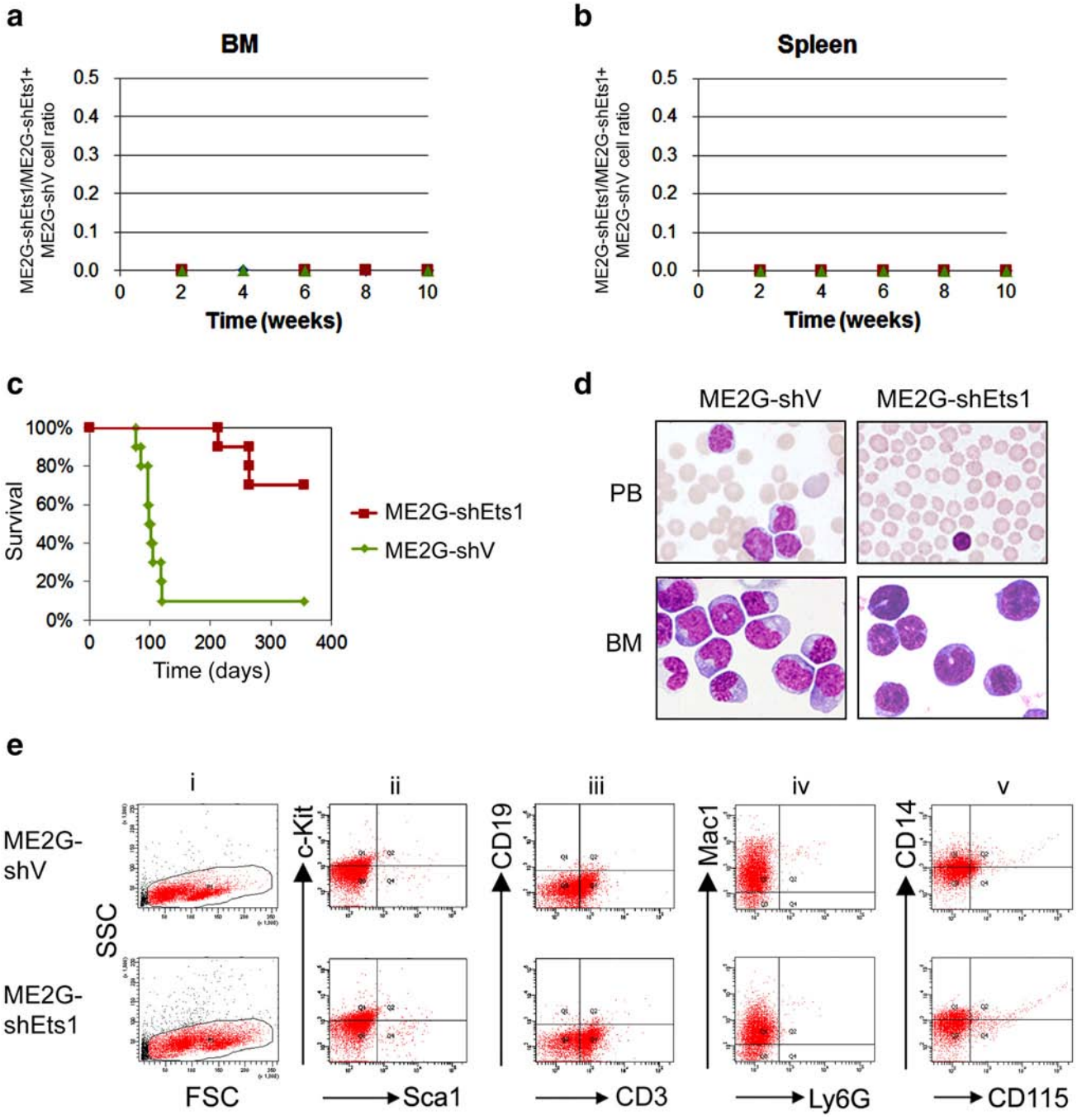

Figure 5. Characteristics of leukemic mice transplanted with *Ets1*-knockdown *MLL/EB1* cells. (A-B) *In vivo* competitive engraftment/clonal expansion of the ME2G-shV and ME2G-shEts1 cells in the BM (A) and spleen (B) of recipient mice. ME2G-shEts1 and ME2G-shV cells were initially mixed at a 1:1 ratio (by cell number). (C) Survival curves of the sublethally irradiated mice ip injected with ME2G-shV or ME2G-shEts1 cells. (D) Liu staining of PB smears (upper panel) or cytospin preparations of BM cells (lower panel) from representative leukemic mice (oil immersion, ×1000). (E) Representative BM flow cytometric analysis of hematopoietic subsets in the ME2G-shV- (upper panel) or ME2G-shEts1- (lower panel) leukemic mice.

Figure 4. Characteristics of *Ets1*-knockdown *MLL/EB1* cells. (A) RT-qPCR (i) and Western blot (ii) analyses of *Ets1* expression level in the lentivirus-transduced ME2G cells. ME2G-shEts1, ME2G cells transfected with lentivirus expressing-shRNA-targeted *Ets1* (TRCN0000042639). ME2G-shV, ME2G cells transfected with blank lentivirus. Error bars indicate SD of mean. (B) Immunofluorescence staining of ME2G-shV and ME2G-shEts1 cells. Cells were stained with anti-Ets1 (left column) or DAPI (middle column), and a merged image (right column). (C) Cytological and (D) immunophenotypic characteristics of ME2G-shV and ME2G-shEts1 cells. (E) RT-qPCR analysis of CD115, *Cybb*, and CD68 expression in ME2G-shV and ME2G-shEts1 cells. (F) Liu staining of ME2G-shV and ME2G-shEts1 cells cultured in the medium containing M-CSF (oil immersion, ×1000). (G) Growth curve and (H) cell apoptosis analyses of ME2G-shV and ME2G-shEts1 cells cultured in the medium containing IL3. Error bars indicate SD of mean (G).

cells in the medium supplemented with lymphoid differentiation-inducing cytokines. Recently, it had been reported that BM stroma was required for normal B-cell development and lymphoid malignancies[25]; hence, there could be a possibility that our *in vitro* culture condition was not enough to sustain the growth of lymphoid leukemia cells. On the other hand, a recent report had shown that *MLL* fusions could target multipotent hematopoietic stem and progenitor cells to induce mixed-lineage leukemia as well as lineage switch from B-ALL to AML or vice versa in acute leukemia patients with *MLL* rearrangements.[26] Unfortunately, our study patient left the hospital without undergoing treatment[17]; therefore, follow-up samples were not available to assess whether linage conversion occurred in the patient.

The low leukemogenic potential and various cell differentiation- and apoptosis-associated characteristics of *MLL/EB1* cells in comparison with *MLL/AF10(OM-LZ)* cells implicated that there may be different target genes downstream of *MLL/EB1*. Comparative transcriptome analysis identified 318 differentially expressed genes between *MLL/EB1* cells and *MLL/AF10(OM-LZ)* cells. The enrichment of the genes involved in the biological processes of cell differentiation, proliferation/apoptosis, homing/recruitment, and immune response was consistent with our experimental observations. From the differentially expressed genes, we identified *Ets1,* a known MLL and MLL/AF9-bound gene, which was selectively upregulated by *MLL/EB1* and played critical roles in *MLL/EB1*-mediated leukemic transformation. *Ets1* gene encodes a widely expressed transcription factor involving in many biological processes, including embryogenesis, vasculogenesis, angiogenesis, proliferation, hematopoiesis, and tumorigenesis.[27–30] In hematopoiesis, *Ets1* was involved in decisions governing the fate of B-/T-lymphocytic cells and megakaryocyte/erythrocyte progenitor cells as well as in the development of natural killer cells, granulocytes, and macrophages.[31–35] Ets1/Ets2 and METS/DP103 function cooperatively in linking terminal macrophage differentiation to cell cycle arrest.[33] Our results demonstrated that the knockdown of *Ets1* expression in *MLL/EB1* cells reduced monocytic gene expression, blocked M-CSF–induced terminal macrophage differentiation, and decreased the frequency of cell apoptosis. These results indicated that *Ets1* in *MLL/EB1* leukemia cells, like in macrophages, linked macrophage differentiation and cell cycle arrest (cell apoptosis). On the other hand, the knockdown of *Ets1* expression in *MLL/EB1* cells strongly hampered cell engraftment to BM/spleen and leukemia development and consequently prolonged the survival of leukemic mice. These results uncovered the dual roles of *Ets1*; it was found to not only attenuate leukemia cell growth but also promote tumorigenesis. Similar observation was reported that *Ets1* controls balance between cell invasion and growth in breast cancer.[36]

Gene amplification and missense mutations of *ETS1* have been detected in patients with marginal zone B cell lymphoma and diffuse large B cell lymphoma (7.9%-20.8%),[37–39] but no direct involvement of *Ets1* was reported in leukemia. More AML samples showing *MLL* fusion with dimerization domain-containing partner genes will be needed to evaluate whether *ETS1* overexpression is common in such type of AML patients. Moreover, Thiel et al. (2010) proposed that wild-type *MLL* is required for *MLL* fusion-induced leukemogenesis.[40] The molecular mechanism governing the selective upregulation of *Ets1* by *MLL* in association with *MLL/EB1* and the tumorigenic role of *Ets1* in *MLL/EB1*-induced leukemic development remain to be explored.

Supplementary data to this article can be found online at https://doi.org/10.1016/j.neo.2019.03.006.

Acknowledgement

This work was supported by grants from the Ministry of Science and Technology, Taiwan (MOST 103-2320-B-182A-005), and Chang Gung Memorial Hospital, Taiwan (CMRPG3B1421-3, CMRPG 3E0301-3, CMRPG3E1391-3). We thank Ms. Yu-Ju Lin and Mr. Jun-Wei Huang for technical assistance in all the experiments.

Conflict-of-interest disclosure: The authors declare no competing financial interests.

References

[1] Dimartino JF and Cleary ML (1999). Mll rearrangements in haematological malignancies: lessons from clinical and biological studies. *Br J Haematol* **106**, 614–626.
[2] Pui CH, Behm FG, Downing JR, Hancock ML, Shurtleff SA, Ribeiro RC, Head DR, Mahmoud HH, Sandlund JT, and Furman WL, et al (1994). 11q23/MLL rearrangement confers a poor prognosis in infants with acute lymphoblastic leukemia. *J Clin Oncol* **12**, 909–915.
[3] Rubnitz JE, Link MP, Shuster JJ, Carroll AJ, Hakami N, Frankel LS, Pullen DJ, and Cleary ML (1994). Frequency and prognostic significance of HRX rearrangements in infant acute lymphoblastic leukemia: a Pediatric Oncology Group study. *Blood* **84**, 570–573.
[4] Meyer C, Burmeister T, Groger D, Tsaur G, Fechina L, Renneville A, Sutton R, Venn NC, Emerenciano M, and Pombo-de-Oliveira MS, et al (2018). The MLL recombinome of acute leukemias in 2017. *Leukemia* **32**, 273–284.
[5] Daser A and Rabbitts TH (2005). The versatile mixed lineage leukaemia gene MLL and its many associations in leukaemogenesis. *Semin Cancer Biol* **15**, 175–188.
[6] Krivtsov AV and Armstrong SA (2007). MLL translocations, histone modifications and leukaemia stem-cell development. *Nat Rev Cancer* **7**, 823–833.
[7] Meyer C, Kowarz E, Hofmann J, Renneville A, Zuna J, Trka J, Ben Abdelali R, Macintyre E, De Braekeleer E, and De Braekeleer M, et al (2009). New insights to the MLL recombinome of acute leukemias. *Leukemia* **23**, 1490–1499.
[8] Bernt KM, Zhu N, Sinha AU, Vempati S, Faber J, Krivtsov AV, Feng Z, Punt N, Daigle A, and Bullinger L, et al (2011). MLL-rearranged leukemia is dependent on aberrant H3K79 methylation by DOT1L. *Cancer Cell* **20**, 66–78.
[9] Zeisig BB, Garcia-Cuellar MP, Winkler TH, and Slany RK (2003). The oncoprotein MLL-ENL disturbs hematopoietic lineage determination and transforms a biphenotypic lymphoid//myeloid cell. *Oncogene* **22**, 1629–1637.
[10] Xu J, Li L, Xiong J, denDekker A, Ye A, Karatas H, Liu L, Wang H, Qin ZS, Wang S, Dou Y. MLL1 and MLL1 fusion proteins have distinct functions in regulating leukemic transcription program. Cell Discov 2016;2: 16008.
[11] Kar A and Gutierrez-Hartmann A (2013). Molecular mechanisms of ETS transcription factor-mediated tumorigenesis. *Crit Rev Biochem Mol Biol* **48**, 522–543.
[12] So CW, Karsunky H, Passegue E, Cozzio A, Weissman IL, and Cleary ML (2003). MLL-GAS7 transforms multipotent hematopoietic progenitors and induces mixed lineage leukemias in mice. *Cancer Cell* **3**, 161–171.
[13] So CW, Lin M, Ayton PM, Chen EH, and Cleary ML (2003). Dimerization contributes to oncogenic activation of MLL chimeras in acute leukemias. *Cancer Cell* **4**, 99–110.
[14] Eguchi M, Eguchi-Ishimae M, and Greaves M (2004). The small oligomerization domain of gephyrin converts MLL to an oncogene. *Blood* **103**, 3876–3882.
[15] Liedtke M, Ayton PM, Somervaille TC, Smith KS, and Cleary ML (2010). Self-association mediated by the Ras association 1 domain of AF6 activates the oncogenic potential of MLL-AF6. *Blood* **116**, 63–70.
[16] So CW, Karsunky H, Wong P, Weissman IL, and Cleary ML (2004). Leukemic transformation of hematopoietic progenitors by MLL-GAS7 in the absence of Hoxa7 or Hoxa9. *Blood* **103**, 3192–3199.
[17] Fu JF, Hsu HC, and Shih LY (2005). MLL is fused to EB1 (MAPRE1), which encodes a microtubule-associated protein, in a patient with acute lymphoblastic leukemia. *Genes Chromosomes Cancer* **43**, 206–210.
[18] Su LK and Qi Y (2001). Characterization of human MAPRE genes and their proteins. *Genomics* **71**, 142–149.
[19] Rehberg M and Graf R (2002). Dictyostelium EB1 is a genuine centrosomal component required for proper spindle formation. *Mol Biol Cell* **13**, 2301–2310.
[20] Slep KC, Rogers SL, Elliott SL, Ohkura H, Kolodziej PA, and Vale RD (2005). Structural determinants for EB1-mediated recruitment of APC and spectraplakins to the microtubule plus end. *J Cell Biol* **168**, 587–598.

[21] Fu JF, Hsu CL, and Shih LY (2010). MLL/AF10(OM-LZ)-immortalized cells expressed cytokines and induced host cell proliferation in a mouse bone marrow transplantation model. *Int J Cancer* **126**, 1621–1629.

[22] Fu JF, Yen TH, Chen Y, Huang YJ, Hsu CL, Liang DC, and Shih LY (2013). Involvement of Gpr125 in the myeloid sarcoma formation induced by cooperating MLL/AF10(OM-LZ) and oncogenic KRAS in a mouse bone marrow transplantation model. *Int J Cancer* **133**, 1792–1802.

[23] Fu J-F, Liang S-T, Huang Y-J, Liang K-H, Yen T-H, Liang D-C, and Shih L-Y (2017). Cooperation of MLL/AF10(OM-LZ) with PTPN11 activating mutation induced monocytic leukemia with a shorter latency in a mouse bone marrow transplantation model. *Int J Cancer* **140**, 1159–1172.

[24] Kogan SC, Ward JM, Anver MR, Berman JJ, Brayton C, Cardiff RD, Carter JS, de Coronado S, Downing JR, and Fredrickson TN, et al (2002). Bethesda proposals for classification of nonlymphoid hematopoietic neoplasms in mice. *Blood* **100**, 238–245.

[25] Sangaletti S, Tripodo C, Portararo P, Dugo M, Vitali C, Botti L, Guarnotta C, Cappetti B, Gulino A, and Torselli I, et al (2014). Stromal niche communalities underscore the contribution of the matricellular protein SPARC to B-cell development and lymphoid malignancies. *Oncoimmunology* **3**e28989.

[26] Dorantes-Acosta E and Pelayo R (2012). Lineage switching in acute leukemias: a consequence of stem cell plasticity? *Bone Marrow Res* **2012**, 406796.

[27] Dittmer J (2003). The biology of the Ets1 proto-oncogene. *Mol Cancer* **2**, 1–21.

[28] Dittmer J (2015). The role of the transcription factor Ets1 in carcinoma. *Semin Cancer Biol* **35**, 20–38.

[29] Findlay VJ, LaRue AC, Turner DP, Watson PM, and Watson DK (2013). Understanding the role of ETS-mediated gene regulation in complex biological processes. *Adv Cancer Res* **119**, 1–61.

[30] Garrett-Sinha LA (2013). Review of Ets1 structure, function, and roles in immunity. *Cell Mol Life Sci* **70**, 3375–3390.

[31] Bories J-C, Willerford DM, Grevin D, Davidson L, Camus A, Martin P, Stehelin D, and Alt FW (1995). Increased T-cell apoptosis and terminal B-cell differentiation induced by inactivation of the Ets-1 proto-oncogene. *Nature* **377**, 635–638.

[32] Barton K, Muthusamy N, Fischer C, Ting C-N, Walunas TL, Lanier LL, and Leiden JM (1998). The Ets-1 transcription factor is required for the development of natural killer cells in mice. *Immunity* **9**, 555–563.

[33] Klappacher GW, Lunyak VV, Sykes DB, Sawka-Verhelle D, Sage J, Brard G, Ngo SD, Gangadharan D, Jacks T, and Kamps MP, et al (2002). An induced Ets repressor complex regulates growth arrest during terminal macrophage differentiation. *Cell* **109**, 169–180.

[34] Lulli V, Romania P, Morsilli O, Gabbianelli M, Pagliuca A, Mazzeo S, Testa U, Peschle C, and Marziali G (2006). Overexpression of Ets-1 in human hematopoietic progenitor cells blocks erythroid and promotes megakaryocytic differentiation. *Cell Death Differ* **13**, 1064–1074.

[35] Lulli V, Romania P, Riccioni R, Boe A, Lo-Coco F, Testa U, and Marziali G (2010). Transcriptional silencing of the ETS1 oncogene contributes to human granulocytic differentiation. *Haematologica* **95**, 1633–1641.

[36] Furlan A, Vercamer C, Bouali F, Damour I, Chotteau-Lelievre A, Wernert N, Desbiens X, and Pourtier A (2014). Ets-1 controls breast cancer cell balance between invasion and growth. *Int J Cancer* **135**, 2317–2328.

[37] Morin RD, Mendez-Lago M, Mungall AJ, Goya R, Mungall KL, Corbett RD, Johnson NA, Severson TM, Chiu R, and Field M, et al (2011). Frequent mutation of histone-modifying genes in non-Hodgkin lymphoma. *Nature* **476**, 298–303.

[38] Pasqualucci L, Trifonov V, Fabbri G, Ma J, Rossi D, Chiarenza A, Wells VA, Grunn A, Messina M, and Elliot O, et al (2011). Analysis of the coding genome of diffuse large B-cell lymphoma. *Nat Genet* **43**, 830–837.

[39] Flossbach L, Holzmann K, Mattfeldt T, Buck M, Lanz K, Held M, Moller P, and Barth TF (2013). High-resolution genomic profiling reveals clonal evolution and competition in gastrointestinal marginal zone B-cell lymphoma and its large cell variant. *Int J Cancer* **132**, E116-127.

[40] Thiel AT, Blessington P, Zou T, Feather D, Wu X, Yan J, Zhang H, Liu Z, Ernst P, and Koretzky GA, et al (2010). MLL-AF9–induced leukemogenesis requires coexpression of the wild-type Mll allele. *Cancer Cell* **17**, 148–159.